International Journal of Geophysics and Geochemistry
2016; 3(3): 25-37
http://www.aascit.org/journal/ijgg
ISSN: 2381-1099 (Print); ISSN: 2381-1102 (Online)

American Association for Science and Technology

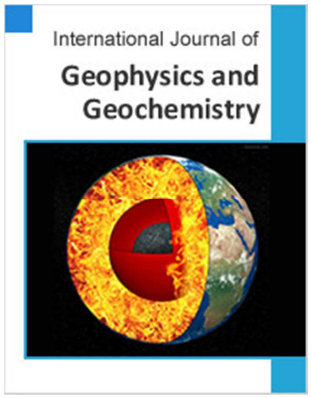

Keywords
ERC,
Red Sea,
Essexite Gabbros,
Miaskitic

Received: February 12, 2016
Accepted: March 2, 2016
Published: May 25, 2016

Geology, Petrography and Geochemistry of El-kahfa Ring Complex, South Eastern Desert, Egypt

Hussein A. Hegazy[1], Andrei A. Arzamastsev[2], Eman Saad[1]

[1]Geology Department, Faculty of Science, Assiut University, Assiut, Egypt
[2]Institute of Precambrian Geology and Geochronology, Russian Academy of Sciences, Moscow, Russia

Email address
emangelogist@yahoo.com (E. Saad)

Citation
Hussein A. Hegazy, Andrei A. Arzamastsev, Eman Saad. Geology, Petrography and Geochemistry of El-kahfa Ring Complex, South Eastern Desert, Egypt. *International Journal of Geophysics and Geochemistry.* Vol. 3, No. 3, 2016, pp. 25-37.

Abstract
El kahfa Ring Complex (ERC) is a member of an alkaline province including complexes of similar size, structure and composition which crop out along the western margin of the Red Sea in Egypt. ERC (5x6 km) occurs as oval intrusion, rising up to 1018 m.a.s.l. at the intersection of latitude 24° 08' 18″and longitude 34° 38' 55″, belongs to the youngest group of Phanerozoic ring complexes having an emplacement age of 92±5Ma (Lutz et al., 1988; Serencsits et al., 1981). It is related to structural lineament trending N 30º W parallel to the Red Sea and was controlled by pre-existing deep crustal lines of weakness in the basement complex. Field investigation revealed that ERC is composed of two intrusive phases, i.e. oldest one represents by essexite gabbros, and the later phase of syenitic rocks. The syenites formed the inner zone are highly sheared undersaturated syenites (i.e. Litchfieldite and cancrinite syenites) grading into quartz syenites, while the outer ring massif is composed of massive alkaline syenites with less of quartz syenites. The extrusive rocks of trachyte, basalt and rhyolite present as plugs, sheets and ring dykes. The mineralogical and chemical features show that these rocks belong to anorogenic interplate A-type alkaline suite (i.e. enriched in alkalis and HFS elements, Nb, Ta, Zr, Hf, Y, HREE) and peralumineous in nature. The Y/Nb and Ce/Nb ratios suggest fractional crystallization of primary source of picritic basalt magma in the asthenospheric mantle. The calculated agpaitic coefficient values show that the alkaline rock samples of El Kahfa area are of miaskitic type with some tendencies to possess an intermediate alkaline affinity. Open-system processes by which nepheline syenitic magma undergo assimilation of silica- rich crustal material (crustal contamination) and fractional crystallization have been suggested. It is believed that under these conditions undersaturated magma evolves across the feldspar join and become oversaturated.

1. Introduction

The great diversity of alkaline rocks, with their relatively exotic minerals, has attracted the interest of petrologists due to their large containing of Nb, Ta, Zr, Y, Th, Cu ore deposits. The importance of academic research on these rocks is thus clear. There is, however also a commercial aspect, is so far as they are an increasingly importance source of a wide range of industrial raw materials.

The occurrence and the tectonic environment of the Egyptian alkaline ring complexes

have been reviewed by several workers (e.g. (de Gruyter and Vogel, 1981; EL Ramly et al., 1969; 1971; EL Ramly and Hussein, 1985). The alkaline magmatism occur in a distinctive regime and similar to these occurring elsewhere (Neary et al., 1976) but the Egyptian complexes show activity over a much longer period of time ranging from Paleozoic up to Cretaceous. A glance at Eastern Desert, there is no clear geographic pattern to the ages, while some complexes appear to be aligned along structural weakness. This suggests its relation with the cyclic formation of supercontinent and the generation of alkaline magmas at different mantle levels (Balashov and Glaznev, 2006).

The geological setting of these alkaline provinces shows that their location is not random. Garson and Krs (1976) proposed that most of the alkaline ring complexes of the Eastern Desert are controlled by two sets of major structural lineament. One of them trends N 60° E, the other trend N 30° W and is a deep-seated block- fault zone parallel to the Red Sea to which ERC is associated. El Kahfa ring complex belongs to the youngest group having age 92 ± 5 Ma. (Lutz et al., 1988; Serencsits et al., 1981).

2. Field Investigations

El kahfa Ring Complex (5x6 km) is located to the south of Abu Khruq ring complex and forms a steeply conical hill rising up to 1018 m.a.s.l. (Fig. 1). This province is mainly composed of essexitic gabbros and syenitic rocks as well as extrusive rocks of trachyte, rhyolite and basanite. The essexitic gabbros occur as small hills at the entrance of the wadi (Fig 2A) and represent the oldest intrusive phase; they are intruded later by syenitic rocks. The essixites are medium to coarse-grained massive rocks with dark colour and weathered into spheroidal bodies of different sizes. White greenish colour syenites are observed intruded into these gabbros at some places.

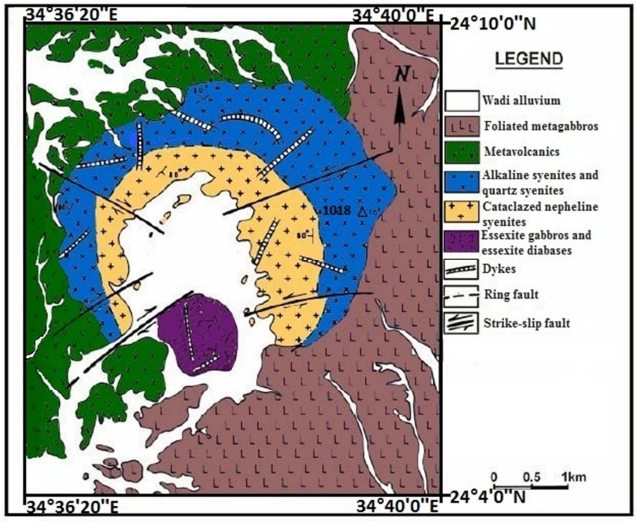

Fig. 1. *Modified geologic map of G. El Kahfa ring complex after (EL Ramly et al., 1971).*

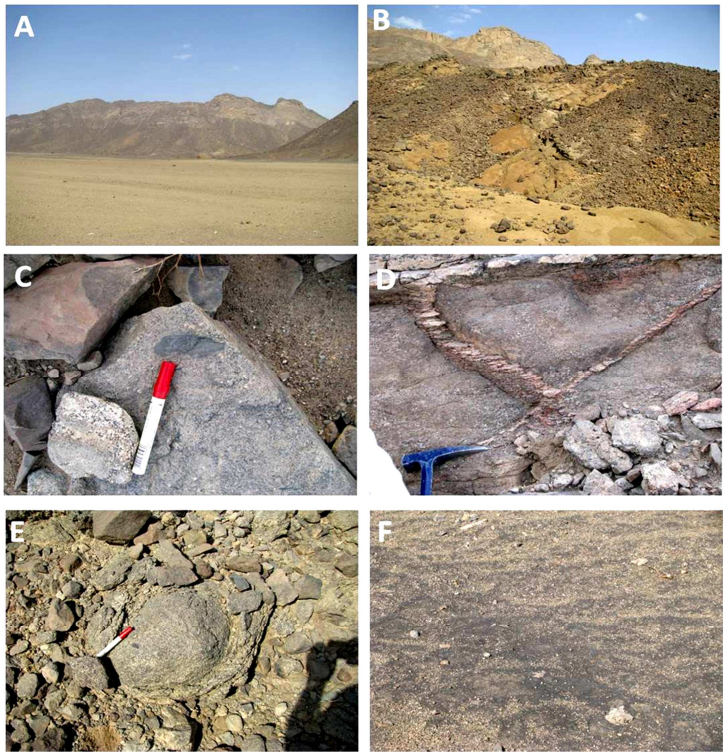

Fig. 2. *A- A view looking east, showing Gabal El Kahfa with small hill of alkaline essexite gabbro on the right side, B- A view showing the two phases of syenitic rocks the sheared inner rim and the outer rim with the high peak of G. El Kahfa C- A close up view showing mafic xenoliths in syenitic rocks, D- A close up view showing pegmatite veins cutting the syenitic rocks, E- A close up view showing spheroid exfoliation of syenitic bodies and F- Black sand grains enriched in radioactive products in the land of G. El Kahfa.*

The syenitic rocks are emplaced during two phases of igneous activity; the oldest one forms the sheared inner rim (Fig. 2B). These highly sheared nepheline syenite is grading into quartz-syenites. They are closely associated in the field and forming the foreland oldest ring. The massive rocks of the high outer ring of light color represent the youngest phase of alkaline syenites with less of quartz syenites. The present relief of the complex is accounted for by the development of the ring faults, the moderate subsidence of the inner ring and the intensive uplifting of the alkaline syenites forming the outer ring. These syenites contain several mafic xenoliths of different sizes and shapes showing some degree of digestion (Fig. 2C). A number of pegmatitic veins of different sizes are associated with the syenite rocks, particularly the oldest phase (Fig. 2D), sometimes syenitic bodies show weathered surfaces “Spheroid Exfoliation" (Fig. 2E).

Of specific field observation, sand grains of black colour are believed as formed at the expense of nepheline syenites enriched in radioactive products of monazite, thorite and high grade graphite deposits (Fig. 2F). Several types of rhyolite and basaltic dykes are shown cutting the both phases of syenites. The dykes are generally thin (av. 60cm) and of limited extent.

3. Petrography

Petrographically, the rocks of El Kahfa ring complex represented mainly by syenitic rocks and less abundant essexitic gabbros as well as minor volcanic varieties (i.e. alkali rhyolite, alkali trachyte and basanite).

A Essexite gabbros

These rocks are medium to coarse-grained, dark grey in colour and essentially consist of zoned plagioclase (Fig. 3A), alkali feldspar and interstitial patches of altered nepheline and analcime. The plagioclase occurs as tabular subhedral crystals; usually have labradorite range (An 57%). Alkali feldspar represents by orthoclase microperthite occurs as wedge-shaped areas with bulk compositions ranging from approximately Or 45 to Or 65. Among the mafic minerals, these rocks contain one principal pyroxene phase e.g. Ca-rich augite although some rock samples contain minor acmite, either in the groundmass or rimming more Ca-rich phenocrysts. The pyroxene crystals usually neutral, grey green or brownish color, sector zonng as well as color zoning are common; the various zones often tend to be outlined by opaque oxide inclusions. The Ca-rich pyroxene is rimmed by green acmitic pyroxene especially where the crystals abut areas of nepheline or analcime. Brown hornblende is almost invariably present. Nepheline forms rectangular or hexagonal crystals and have highly sodic compositions close to Ne 90. Analcime is a common accessory mineral, its well-defined euhedral phenocrysts provide the most convinencing textural evidences for forming a primary origin (see Peters et al., 1966). Iron-titanium oxides are the most common accessories as well as apatite and sphene.

B Syenites

Two main types of syenitic rocks depending on the presence of nepheline are investigated.

1. Nepheline-bearing syenite

This variety is discriminated into two types;

a Albite-rich nepheline syenite (Litchfieldite)

This type has two feldspars instead of one and has less than 15% mafic minerals. They are hypidiomorphic granular but occasionally have a distinct trachytoid texture with slender laths of perthitic alkali feldspar set in granular groundmass of albite. Nepheline and its alteration products are less abundant and forms phenocrysts or is part of groundmass components. It often contains inclusions of feldspar and pyroxene, indicating a late origin. The dominant mafic minerals are aegirine-augite, barkevikitic hornblende and biotite. The most common accessories are zircon, calcite, apatite, titanite and fluorite. Sometimes, blue sodalite is present on fractures.

b Cancrinite-Sodalite Syenite

This rock is similar to the previous one which is composed of albite, with small amounts of potassium feldspar, nepheline, biotite, cancrinite and sodalite as primary essential minerals. Microscopically, cancrinite occurs usually in shappless mass, either in, or marginal to nepheline (Fig. 3B). It is colourless and has a perfect prismatic cleavage crystal with high birefringence. The stability of cancrinite is strongly depends on their composition. The temperature of crystallization is determined as 450°-650°C (Edgar, 1964). Sodalite presents as small grey crystals enclose in coarse interlocking crystals of alkali feldspar, aegirine and arfvedsonite. The primary sodalite is distinguished by its content of microlites of aegirine or is dust, while late sodalite is often blue in color and free from such inclusions.

2. Alkaline Syenites

The rocks which forming the outer ring of El Kahfa massif are represented mainly by alkaline syenites, including both quartz-free (Fig. 3C) and quartz-bearing varieties showing corrosion between quartz and alkali feldspars (Fig. 3D). The quartz-bearing alkali syenites is named nordmarkites, whereas the large group of alkali syenites are hard, massive and medium to coarse grained rocks with light grey to buff colors. They are composed mainly of alkali feldspars with less albite (An7-9%), aegirine, and biotite in the form of hypidiomorphic textures. Alkali feldspars are represented by euhedral to subhedral elongated laths of orthoclase microperthites and orthoclase. Apatite, zircon, fluorite and opaque oxides are the main accessories.

3. Quartz syenites

The quartz syenites generally have less than 5% mafic minerals (i.e. aegirine-augite, riebeckite and iron rich biotite). They are hypidiomorphic granular and are mainly composed of tabular microperthite (70%), quartz (20%). The quartz is interstitial or forms crystals in miarolitic cavities (Fig. 3E). Zircon, sphene and iron oxides are the common accessories.

C Alkali trachyte

It is a fine-grained member of buff colour. Microscopically

consists mainly of a phenocrysts of sanidine and oxidized aegirne-augite set in a fluidal ground mass of subparallel sanidine laths (Fig. 3F) with intergranular aegirine-augite, aegirine and iron oxides, plus accessories apatite and sphene. Triangular and polygonal spaces between the sanidine laths are occupied by analcite and sodalite.

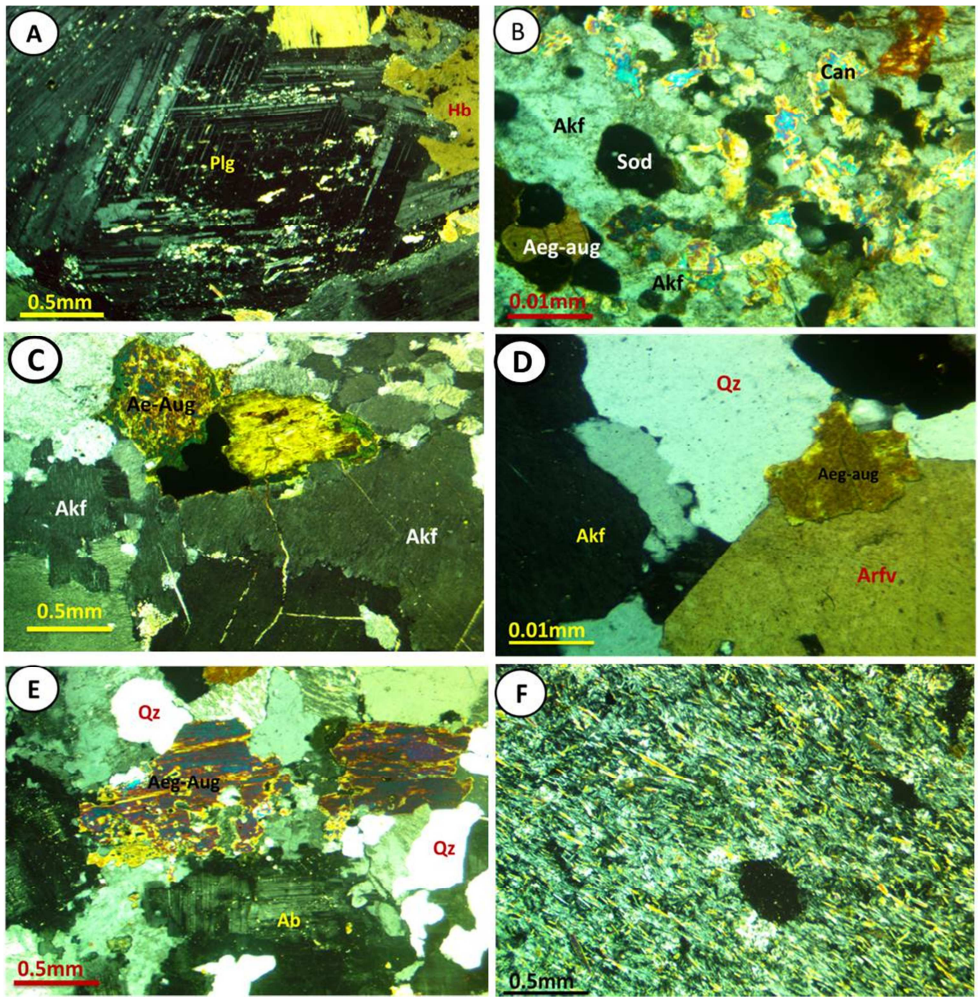

Fig. 3. *A- Photomicrographic show zoned crystal of plagioclase mineral with hornblende of essexite gabbro rock. B- Shappless mass of cancrinite with sodalite, alkali feldspar, aegirine and arfvedsonite of cancrinite-sodalite syenite C- Orthoclase microperthitic with zoned aegirine-augite of alkaline syenite. D- Orthoclase microperthitic with interstitial quartz showing corrosion action in surrounding crystals of alkali pyroxene and alkali amphibole of nordmarkite rock. E- Highly perthitic orthoclase crystals with interstitial quartz and large crystals of aegirine-augite of quartz syenite. F- Fluidal texture of alkali feldspar crystals of trachyte rock. Symboles Plg: plagioclase, Alk: alkali feldspar, Qz: quartz, Ne: nepheline, Aeg-aug: aegirine-augite, Arfv: arfvedsonite, Hb: hornblende, Ab; albite, Sod; sodalite, Can; cancrinite.*

4. Geochemistry

Major Elements

Chemical analyses of 11 representative rock samples of syenites and essexite gabbros from El Kahfa ring complex are done using XRF technique and ICP-MS in labs of Geochemistry of Alkaline Rocks, Institute of Geochemistry, Russian Academy of Sciences, Irkutsk, Russia (Table 1-5). The major oxides of the studied samples (Table 1) display slightly individual trends with relatively broad range of variation; SiO_2 (45.16 to 49.48 and from 53.44 to 63.78%), $A1_2O_3$ (16.14 to 16.97 and from 17.41 to 18.85 wt %), CaO (8.58 to 9.52 and from 0.97 to 5.18 wt %), MgO (4.5 to 5.2 and from 0.04 to 1.2 wt%), while (Na_2O+K_2O) range from (4.56 to 6.11 and from 9.07 to 14.60 wt %), and (Fe_2O_3)t from (11.91 to 12.22 and from 3.41 to 8.77 wt %) in essexite gabbro and syenitic rocks respectively.

On the TAS diagram (Na_2O+K_2O) vs SiO_2 of Wilson et al., (1989) all the analysed samples are plotted in the alkaline field (Fig. 4). On the same diagram, it's clear that the syenitic rocks fall in different syenitic field (i.e. nepheline, alkaline and quartz syenite field), while two of the essexitic gabbro fall in gabbroic field and the third sample fall in syenodiorite field. It is worth to mention that this is confirmed well to petrographic investigation.

It is clear that Al_2O_3 and MgO contents on Harker diagrams (Fig 5A, B respectively) show trends of progressive decreasing with increasing SiO_2. The MgO trend reflects the incorporation of this oxide into early crystallizing phases such as olivine and pyroxene. Essexitic gabbros have the highest CaO contents (on average 9.05 wt %) whereas rocks in the remaining units contain less than 5.18 wt % CaO (Fig 5C), while the relation between silica vs MgO, (Fe_2O_3)t and (Na_2O+K_2O)t show a clear compositional gap between the basic and syenitic rocks (Fig. 5B,

D and E) as previously noted by de Gruyter (1983) and Landoll et al. (1994) which is also evident for other oxides. All rocks are peraluminous in nature, i.e. they all have A/CNK values over one (Fig. 6A) and of sodic type (Fig. 6B). According to Blatt and Tracy (1995) the highly alkali nature of the magma and high concentrations of incompatible elements included small degrees of melting of enriched mantle at great depths (60-100 km or more). According to Bailey and Macdonald, (1970) the agpaitic coefficient can be used as quantitative measure at alkalinity. The calculated agpaitic index ((Na+K)/Al) ranges from 0.38 to 1.13 suggest a miaskitic composition, this is confirmed by plotting the agpaitic index vs SiO_2 (Fig. 6C)

The essexitic samples exhibits low albite normative (on average 20.69%) and therefore have high diopside and anorthite normative (on average 16.76% and 23.18% respectively), while in syenites there are a considerable range in the degree of undersaturation about (1.17 to 17%) nepheline normative in the nepheline syenites (Table 2). It is also clear that the undersaturated syenites contain more normative orthoclase and albite. The alkali syenites have (1.17-6.81%) normative nepheline.

Mg # numbers (Table 3) are generally decrease from essexitic gabbro to syenitic samples (58.44 to 2.92), while the differentiation index show an increase from essexitic gabbros (on average 39.09%) to quartz syenites (73.45%), nepheline syenites (83.16%) and alkali syenites (86.73%).

Table 1. *Major elements compositions of rock samples of El Kahfa ring complex.*

Rock name	Essexite gabbro		Syenodiorite	Nepheline syenite		Alkaline syenite				Quartz syenite	
S. No.	**1**	**2**	**3**	**4**	**5**	**6**	**7**	**8**	**9**	**10**	**11**
SiO_2	45.16	49.48	53.44	59.04	58.09	60.07	59.96	60.33	63.78	55.23	55.51
TiO_2	2.93	1.42	1.73	0.167	0.161	0.47	0.253	0.629	0.318	1.158	1.196
Al_2O_3	16.14	16.97	17.83	18.8	18.15	17.97	18.85	17.41	17.87	17.41	17.79
Fe_2O_3	2.86	5.4	3.87	3.50	4.72	2.62	3.25	3.07	2.38	3.43	3.55
FeO	9.36	6.51	4.90	1.58	1.76	3.04	2.15	2.88	1.03	5.08	4.38
MnO	0.36	0.16	0.146	0.145	0.104	0.15	0.136	0.159	0.072	0.194	0.179
MgO	5.2	4.5	2.455	0.04	0.253	0.46	0.148	0.494	0.214	0.992	1.209
CaO	9.52	8.58	5.181	0.97	2.609	2.26	1.62	2.28	1.04	4.3	3.793
Na_2O	4.03	3.53	6.61	9.8	7.46	6.68	7.87	7.97	7.68	7.69	7.99
K_2O	2.08	1.03	2.464	4.807	4.342	4.51	4.425	3.77	4.917	2.436	2.865
P_2O_5	0.66	0.32	0.36	0.038	0.022	0.11	0.073	0.126	0.035	0.298	0.311
LOI	1.22	1.25	0.25	0.83	2.15	1.15	0.88	0.5	0.5	1.25	0.74
Total	99.52	99.15	99.24	99.72	99.82	99.49	99.62	99.62	99.84	99.47	99.51

Table 2. *The Calculated CIPW norms of the rock samples of El Kahfa ring complex.*

S. No.	Quartz (Q)	Corundum (C)	Orthoclase (Or)	Albite (Ab)	Anorthite (An)	Nepheline (Ne)	Diopside (Di)	Hypersthene (Hy)
1			17.03	11.51	17.44	12.24	21.19	
2	0.42		3.11	29.87	28.91		12.32	13.17
3			14.56	43.21	11.7	6.89	9.46	
4			28.41	37.11		17.78	4.05	
5			25.66	50.57	3.21	6.8	1.36	
6			26.65	54.2	5.73	1.26	4.05	
7			26.15	54.02	3.04	6.81	2.87	
8			22.28	57.62	0.59	5.32	6.43	
9			29.06	62.38		1.17	1.15	
10	10.97		14.4	48.5	5.79		11.52	
11	11.25		16.93	46.85	4.21		10.46	

Table 2. *Continued.*

S. No.	Olivine (Ol)	Magnetite (Mt)	Ilmenite (Il)	Apatite (Ap)	Acmite (Ac)	Na-Metasilicate (Ns)	Wollastonite (Wo)	Hematite (Hm)
1	7.07	4.15	5.57	1.53				
2		7.83	2.31	0.29				
3	3.44	5.61	3.29	0.83				
4	0.66		0.32	0.09	10.13	0.35		
5		5.55	0.31	0.05			3.27	0.89
6	1.51	3.8	0.88	0.26				
7		4.71	0.48	0.17			0.49	
8		4.46	1.19	0.29			0.94	
9		2.63	0.6	0.08	0.39		1.44	0.43
10	1.17	4.98	2.2	0.69				
11	0.94	5.14	2.27	0.72				

Table 3. *Calculated Agpaitic In., D. I. and S. I. of El Kahfa ring complex rock samples.*

S. No.	Solidification Index	Differentiation Index	Color Index	Agpaitic Index	Mg#	Olivine fo
1	33.23	40.78	37.98	0.6	40.35	3.16
2	37	33.4	35.63	0.38	58.44	
3	22.5	64.67	21.8	0.76	43.13	2.18
4	4.69	83.3	15.16	1.13	2.92	0.02
5	12.49	83.03	8.1	0.94	13.78	
6	11.82	82.11	10.25	0.88	18.35	0.39
7	8.39	86.98	8.07	0.94	8.38	
8	11.42	85.22	12.08	0.99	19.78	
9	6.1	92.61	5.21	1	19.62	
10	18.75	71.87	19.87	0.88	23.21	0.37
11	16.8	75.03	18.82	0.91	29.39	0.42

Table 3. *Continued.*

S. No.	Olivine fa	Diopside wo	Diopside en	Dioside fs	Hypersthene en	Hypersthene fs
1	3.92		10.64	4.95	5.58	
2			6.41	4.39	1.51	
3	1.26		4.86	3	1.58	
4	0.64		1.91	0.07	2.07	
5			0.73	0.63		
6	1.12		1.98	0.58	1.49	
7			1.4	0.37	1.1	
8			3.19	1.23	2	
9			0.62	0.53		
10	0.81		5.68	1.95	3.89	
11	0.53		5.25	2.42	2.78	

Solidification Index SI = 100*MgO/ ($MgO+FeO+Fe_2O_3+Na_2O+K_2O$), Differentiation Index DI = Sum of Q, Or, Ab, Ne, Ks and Lc., Color Index Co. I =Total normative mafics; i.e., Di+Hy+Ol+Mt+Hm+Il+Ac. Agpaitic Index Ag.I. =Molar ($Na_2O + K_2O$)/Al_2O_3, Mg# = 100 * Molar Mg/(Mg + Fe)., Olivine forsterite =Wt. % of total rock as normative forsterite in Ol. (Fo + Fa) sum to Ol., Olivine fayalite =Wt. % of total rock as normative fayalite in olivine. (Fo + Fa) sum to Ol., Diopside wollastonite =Wt. % of total rock as normative wollastonite component in Di. (Wo + En + Fs) sum to Di., Diopside enstatite =Wt. % of total rock as normative enstatite component in Di. (Wo + En + Fs) sum to Di., Diopside ferrosilite =Wt. % of total rock as normative ferrosilite component in Di. (Wo + En + Fs) sum to Di., Hypersthene enstatite =Wt. % of total rock as normative enstatite component in Hy. (En + Fs) sum to Hy., Hypersthene ferrosilite =Wt. % of total rock as normative ferrosilite component in Hy. (En + Fs) sum to Hy.

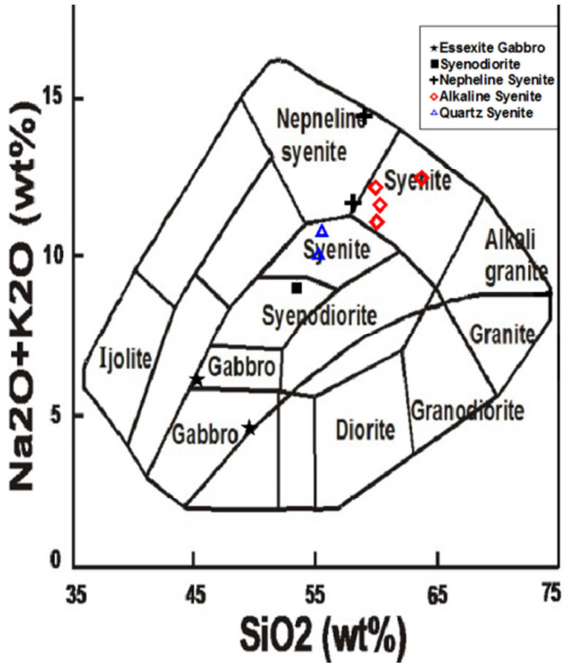

Fig. 4. *TAS diagram for the studied gabbro and syenites of ERC after Cox et al. (1979) adapted by Wilson (1989) for plutonic rocks, the dividing line between alkali and subalkalic magma series is after Miyashiro (1978).*

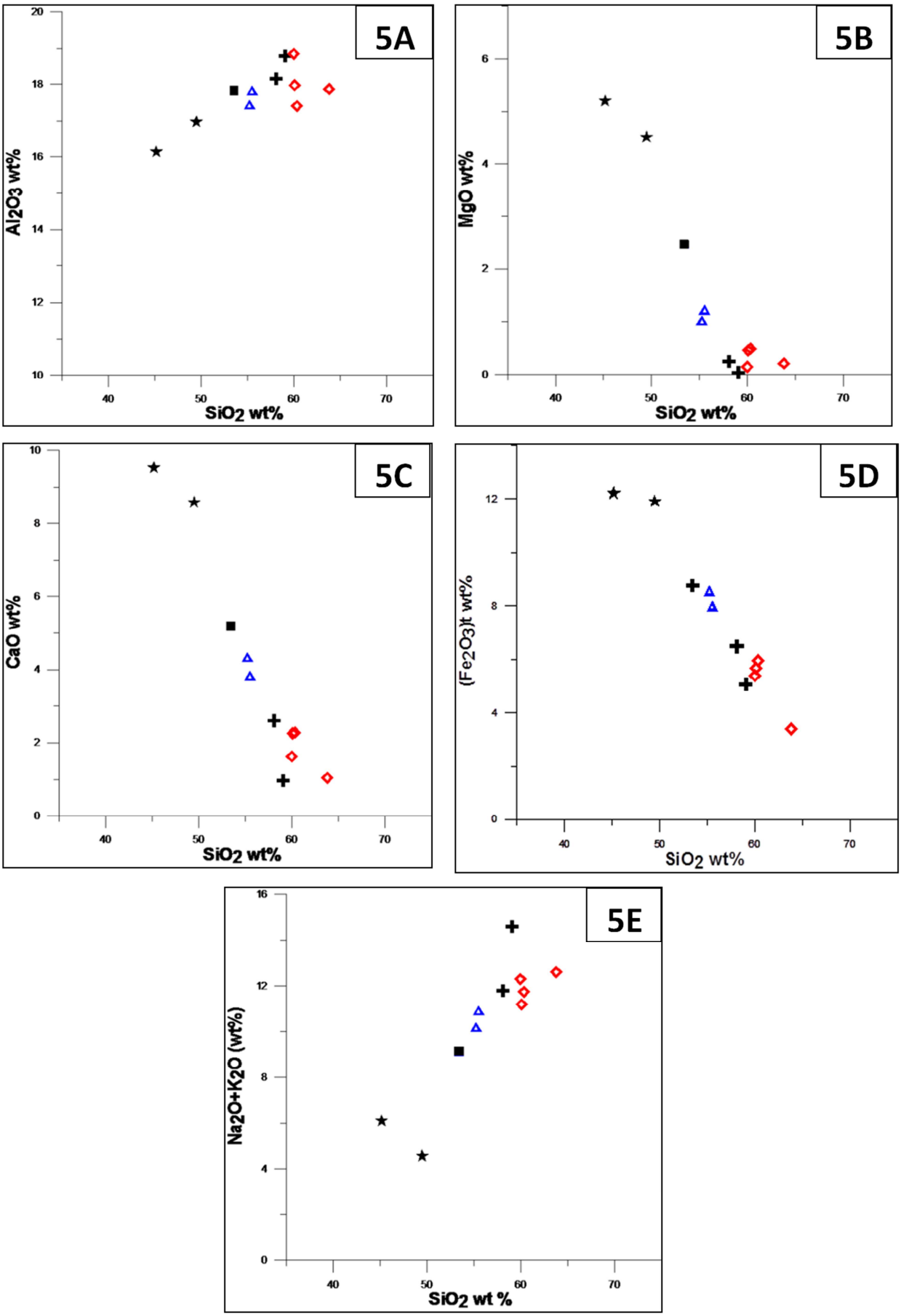

Fig. 5. *Harker variation diagrams of major oxides of ERC symbols as Fig. 4.*

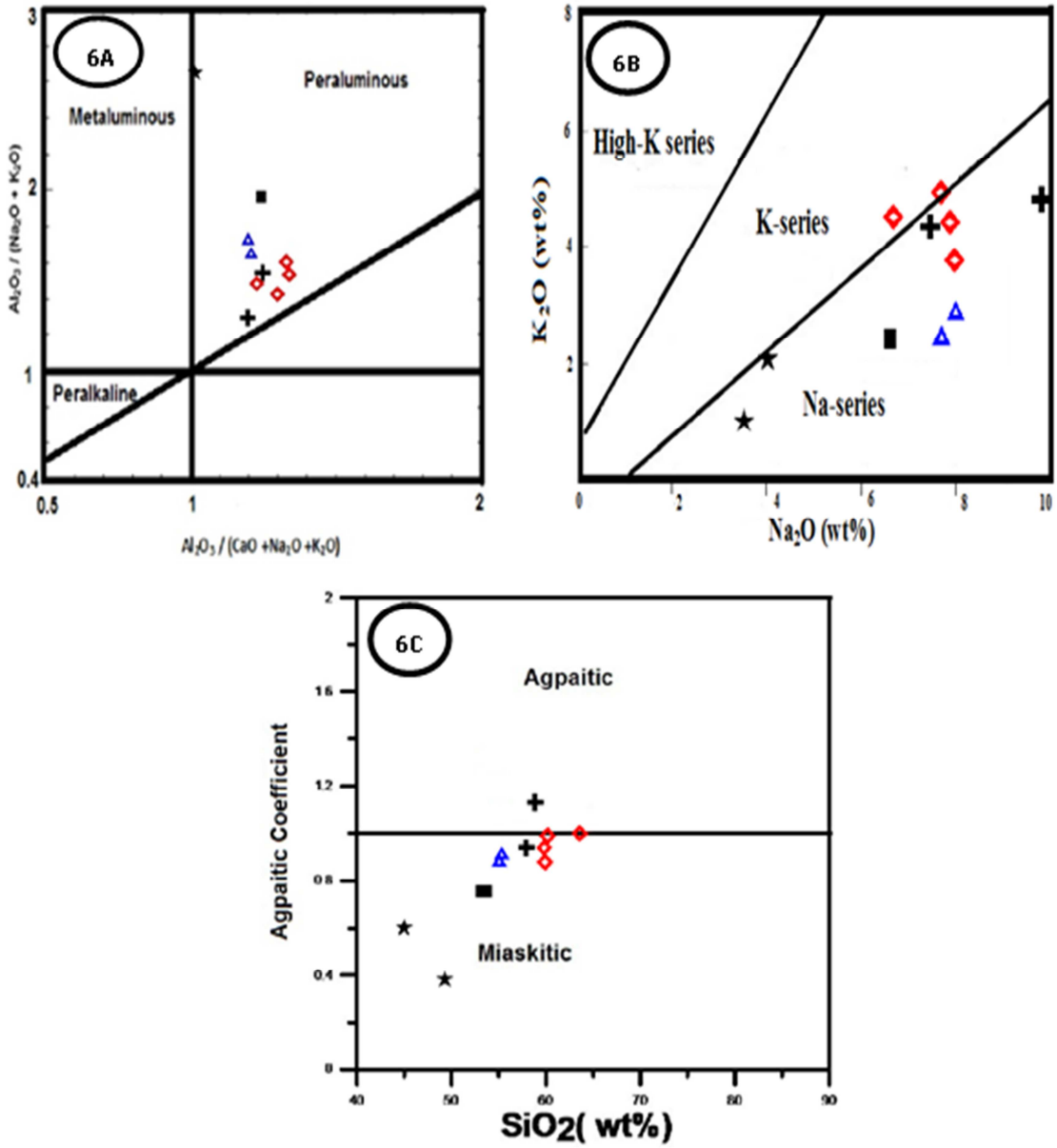

Fig. 6. *A) Alumina saturation diagram after Maniar and Picolli (1989), B) Na_2O wt% vs K_2O wt% diagram after Middlemost (1975) and C) SiO_2 wt% vs agpaitic coefficient of ERC rock samples after Bailey and Macdonald (1970), symbols as Fig. 4.*

Trace elements:

The trace elements data of 10 representative rock samples from El Kahfa are given in (Table 4). Compatible trace elements show sharp decrease from the essexite gabbros to the syenites. V and Cr decrease with increasing the differentiation index for the analyzed samples (i.e. V decrease from 366 to 1 ppm, Cr decreases from 129 to 6 ppm. The low concentration of these elements in the essexitc gabbros, consistent with their derivation from an evolved mafic magma as has been proposed previously by de Gruyter (1981) and Landoll et al. (1994).

These rocks show a Y/Nb values less than 1.2 characteristic features of most alkaline suites (Bonin, 2007). Y is captured in the late apatite and increase as Nb from alkaline syenites to nepheline syenites. The studied samples have geochemical characteristics that are consistent with an intraplate tectonic setting, as viewed on Rb vs (Nb+Y) and Nb vs Y of Pearce et al. (1984). All rock types fall in the anorogenic within plate field (Fig. 7A and 7B).

The basic varieties are enriched in Nb and Zr relative to Y (Table 4). The studied rocks may have high contents of Ba (on average 236 and 532 in essexite gabbro and syenites respectively) and low contents of Rb (on average 46 and 107) in spite of high contents of Na and K. This depletion of Rb may be a result of escape of gas phase in equilibrium with crystallizing magma (Heier, 1964). A similar relationship is observed for Zr (Table 4). Zr appears in a specific phase (i.e. zircon) due to its high radius and charge (Goldschmidt, 1954). It seems likely that zircon is the main carrier of the REE. Ba content increases with differentiation from 358 to 1056 ppm. The sympathitic relationships of Sr and Ba suggest that Ba may also have been added to some samples during hydrothermal

interactions. In syenites Sr does not correlate with SiO_2 or incompatible elements (e.g. Zr, Nb, Ce) indicating to other processes than magma differentiation.

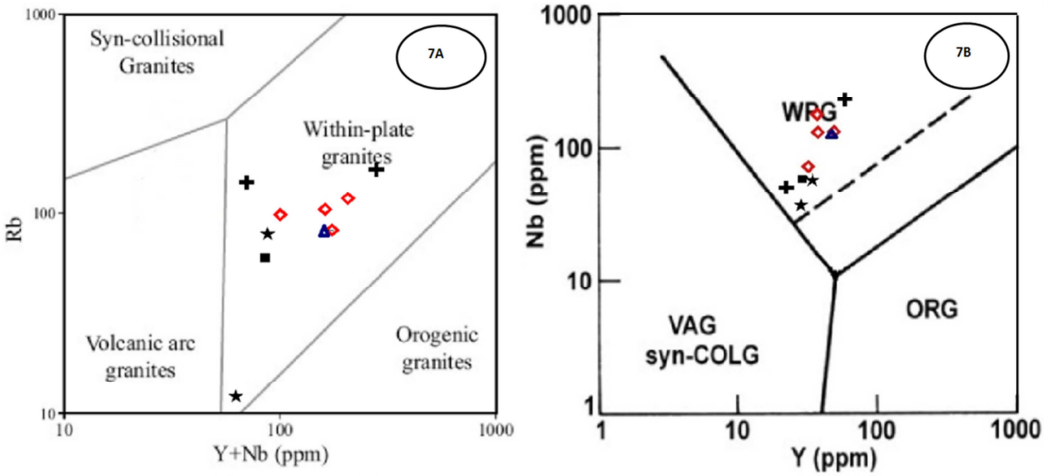

Fig. 7. *A) Rb vs (Nb+Y) and B) Nb vs Y of ERC rock samples indicate within plate granites after Pearce et al. (1984) symbols as Fig. 4.*

Table 4. *Trace elements compositions of Rock samples of G. El Kahfa ring complex.*

Rock name	Essexite gabbro		Syenodiorite	Nepheline syenite		Alkaline syenite				Quartz syenite
Sample No.	**1**	**2**	**3**	**4**	**5**	**6**	**7**	**8**	**9**	**11**
Sc	20	30	9	0.66	0.67	1.49	0.68	3.11	0.98	6.70
Ti	8337	6283	9794	859	796	2515	1417	3259	1643	7097
V	199	366	88	1.26	1.00	2.42	3.31	2.76	1.76	0.95
Cr	75	81	129	30	67	7	46	10	6	26
Co	36	35	21	0.78	0.80	3.13	2.04	3.05	1.73	6.09
Ni	33	41	44	1.60	4.01	2.92	4.62	2.39	2.97	4.87
Cu	27	118	24	9	9	5	12	6	4	10
Zn	272	68	109	148	96	117	134	126	67	132
Ga	28	19	27	37	40	32	32	31	31	31
Rb	79	12	60	167	144	105	119	83	98	82
Sr	625	355	626	23	404	273	179	303	83	580
Y	34	18	29	58	12	37	36	48	32	46
Zr	293	83	441	1606	743	900	1027	931	551	622
Nb	56	36	58	226	49	128	174	129	71	126
Mo	3	1	4	12	10	6	7	6	4	6
Sn	0.30	0.14	0.14	0.19	0.13	7.45	0.31	0.16	0.16	0.23
Cs	1.13	0.35	0.72	1.34	0.74	2.13	1.11	0.57	0.46	1.08
Ba	358	115	675	26	33	435	772	897	359	1056
Hf	5	1	5	16	14	13	14	8	3	10
Ta	3.4	0.2	2.2	15.0	2.5	6.9	9.9	6.9	5.4	6.9
W	0.36	0.07	0.05	0.28	0.13	2.35	0.15	0.14	0.15	0.13
Pb	6	2	6	15	2	9	14	8	9	7
Th	5	1	11	36	4	17	22	13	15	15
U	1.40	0.16	2.40	9.97	0.99	4.64	8.13	2.89	2.31	3.92

Rare Earth Elements (REE):

The REE data of analyzed samples (Table 5) are normalized to condrite values of Sun (1982) (Fig. 8 and 9). The rock samples approximately exhibit depletion in LILE elements (Ba and Sr) but enriched in U, Nb, Ta, Hf and Zr. On the other hand, rocks of the essexite gabbros and syenodiorite are more enriched in both LREE and HREE with a strong negative Hf-anomaly (Fig. 8) with low Yb and Lu, suggesting the presence of residual garnet in the mantle source (Nickel, 1986). Consistent features of nepheline and alkaline syenites spider diagram (Fig. 9) are marked by depletions of Ba, Sr, Ti and HREE and enrichment in some lithophile elements (LILE and LREE). These data suggest a differentiated pattern later that can be associated to metasomatic alterations. Generally, the normalized patterns of the studied rocks show considerable enrichment in both the large–ion lithophile elements and high-field strength elements (LILE and HFSE, respectively), with a lack of a negative Nb-anomaly but have pronounced negative Ba, Sr, and Ti (Fig. 9). These geochemical features are generally believed to be characteristic of igneous rocks occurring in within-plate tectonic environments (Wilson, 1989).

Table 5. *REE elements compositions of rock samples of G. El Kahfa ring complex.*

Rock name	Essexite gabbro		Syenodiorite	Nepheline syenite		Alkaline syenite				Quartz syenite
S. No.	1	2	3	4	5	6	7	8	9	11
La	82	13	109	196	51	79	179	162	83	153
Ce	10	2	12	19	6	144	18	18	9	17
Pr	43	10	45	63	22	16	62	65	31	63
Nd	9	3	9	12	4	55	10	12	6	13
Sm	3	0.9	3	0.6	0.4	10	2	3	1.5	5
Eu	9.4	3	8	11	3	1.4	9	10	5	10
Gd	10	3	8	12	3	8	9	11	6	11
Tb	1.3	0.5	1.1	1.7	0.5	1.3	1.2	1.7	0.9	1.6
Dy	1.3	0.7	1.0	2.0	0.5	7	1.2	1.7	1	1.6
Ho	3.2	2.0	2.8	6.1	1.4	1.3	3.4	4.9	3.1	4.4
Er	0.4	0.3	0.3	0.9	0.2	3.6	0.5	0.6	0.4	0.6
Tm	2.4	1.9	2.0	5.8	2.0	0.5	3.1	3.8	2.7	3.3
Yb	0.3	0.3	0.3	0.8	0.4	3.0	0.4	0.5	0.4	0.5
Lu	5.0	0.6	5	16	14	0.5	15	8	2.5	10

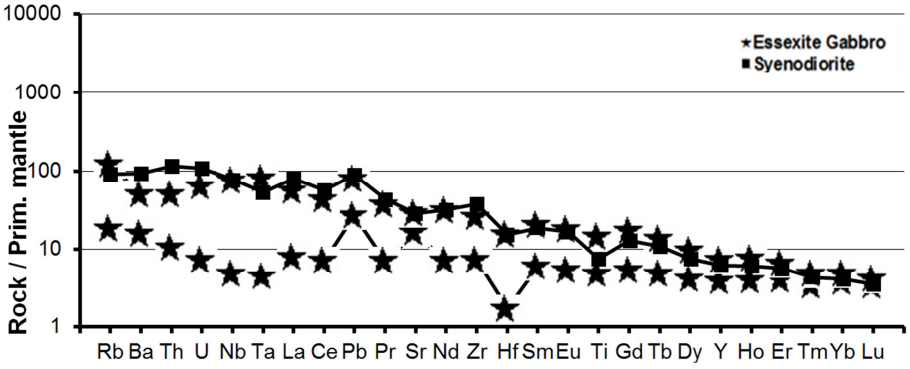

Fig. 8. *Spider diagram of essexite gabbros and syenodiorite of ERC.*

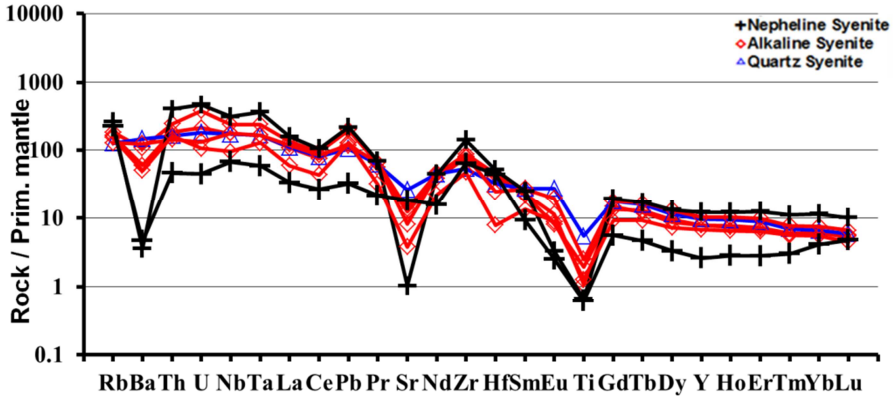

Fig. 9. *Spider diagram of syenitic rocks e of ERC.*

5. Discussion

Origin of the mafic rocks

Mafic rocks (Essexites and Syenodiorites)

The low Mg, Cr, Ni, Co, and V contents observed in essexite gabbros preclude their generation as direct melts from the mantle (McKenzie, 1985); Sun and McDonough, 1989), this is consistent with their derivation from an evolved mafic magma at approximate temperatures of the fraction (about 1200°C on Ab-Iron ratio) (Fig. 10).

According to Kyle (1981), the parental basanitic magma was generated by small amount (1-7%) of partial melting of garnet peridotite source mateials at depth of at least 80 km; while the syenitic and phonolitic rocks evolved as the result of the fractional crystallization and removal of olivine, clinopyroxene, plagioclase, Fe-Ti oxides and apatites. Sepra (1981) has estimated that the amount of heat transported by low-viscosity fluids, fluxing through the upper mantle, is sufficient to generate all the alkaline magma that is believed to form on Earth at the present time.

Cogenetic quartz and nepheline syenites

Two hypotheses have been proposed for cogenetic silica undersaturated and silica-saturated syenitic rocks. The first hypothesis focuses on mechanism to overcome or depress the thermal barrier in Petrogeny's Residue involving volatile (Kogarko, 1974), increasing water pressure and crystal fractionation (Foland and Henderson, 1976; Giret et al., 1980). Studies of Tuttle and Bowen (1958), Hamilton and Mackenzie, (1965) have shown that for composition in the residua system, albite-orthoclase join is a thermal divide at pressures below about 4.2 kbar on which m_s is a thermal low (Fig. 11A). The nepheline syenites (m_n) do plot within a closed thermal depression on the liquidus of petrogeny's residua system. Note that m_o-m_s-m_u is not a straight line (Fig. 11B). The second hypothesis involves open-system processes by which nepheline syenitic magmas undergo assimilation of silica- rich crustal material and fractional crystallization (Harris et al., 1999). Foland et al. (1993) proved that quartz - bearing syenitic melts can be produced from silica-undersaturated syenitic magmas through a process of combined assimilation and fractional crystallization (AFC). They demonstrated that under conditions of open-system assimilation of siliceous crustal rock felsic magmas albite crosses the thermal divide represented by alkali feldspar join in petrogeny's residua.

Landoll et al. (1994) suggested that crustal contamination was important in determining the degree of silica saturation. He mentioned that the open-system contamination processes provide a mechanism for an undersaturated magma to evolve across the feldspar-join and become oversaturated.

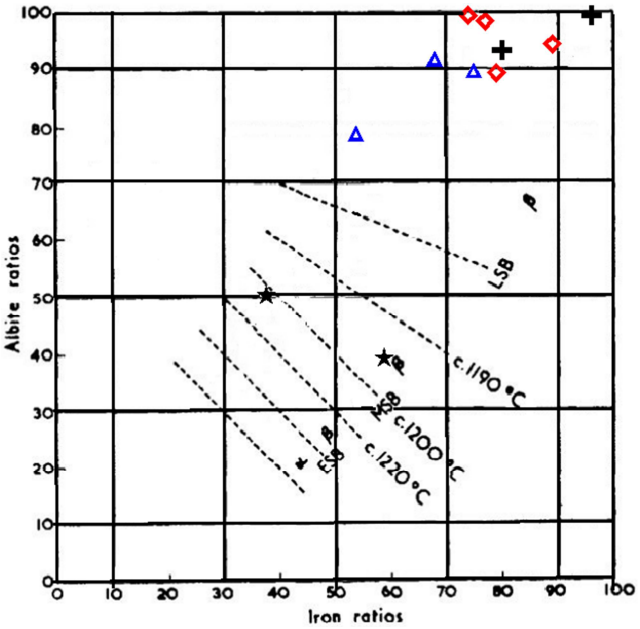

Fig. 10. *Albite ratio vs iron ratio for ERC rock samples after Yoder and Tilley, (1962) Symbols as Fig. 4*

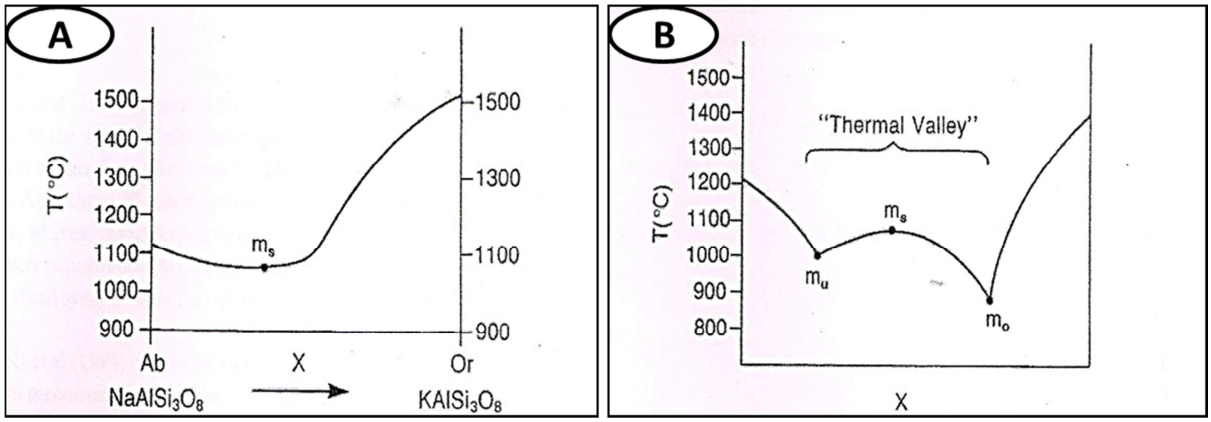

Fig. 11. *Cross section of the liquidus of petrogeny´s residua system along the line Ab-Or (A) and through points m_o-m_s-m_u (the thermal valley) (B), revealing that m_s is a thermal low along Ab-Or, but a high along the thermal valley. Note that m_o-m_s-m_u is not a straight line (Fudali, 1963).*

Mechanism of formation

When reviewing the modal of the mechanism of formation of this ring complex, the following points can be stated

1. In areas of crustal arching, volatile concentration and heat focusing may occur. The melt by diapiric action rose slowly into the base of crust and produce the more silicic magma (rhyolite and trachyte).
2. Differentiation, accompanied by some assimilation, probably produced intermediate syenitic rocks. Isotopic data revealed a possibility that the crustal contamination played a role in the petrogenesis of quartz-bearing syenites at the expense of silica undersaturated syenitic magma.
3. Cauldron subsidence would take place only if there was a large volcanic cone. The formation of the ring intrusion and that of most of the ring dykes is related to the Cauldron subsidences and the passive infilling of the released sparse with magma.
4. On entering the brittle zone of the upper crust diapiric movements would have been retarded which led to a slow buildup of fluid pressure and caused tension fractures focused on the arrested diapirs –break through to the surface.
5. Conical intrusions and both conical and radial dykes were formed during the active upward movements of the alkaline magmas, which overcome the weight of the roof rock.
6. Finally, it should however be obvious to interested

reader that the Egyptian alkaline ring complexes need more detailed study before the origin of these rocks types can be completely understood; Mainwhile, the petrogenetic modal outlined above should provide a framework for subsequant modification and improvement.

6. Conclusions

The main conclusions that are derived from the present work can be summarized as follows:

1. The El Kahfa ring complex is a ploy phases intrusion consists of two comagmatic rock series i.e. essexitic gabbros and silica-undersaturated to saturate evolved syenitic rocks.
2. The Chemical data revealed that the studied alkaline ring complex represents a phanerozoic anorogenic, within-plate magmatism and were derived from the upper mantle by partial melting at approximate temperature of the fractionation (about 1200°C), while the more felsic varieties evolved as the result of the fractional crystallization.
3. The calculated An % content in plagioclase shows that the El Kahfa syenites have oligoclase type.
4. The calculated agpaitic coefficient values show that the rocks of El-kahfa area are of miaskitic type, with some tendencies to possess an intermediate alkaline affinity of sodic series.
5. All the studied rocks approximately exhibit depletion in LIL elements e.g. Ba and Sr, but enriched in U, Ta, Nb, and Zr.
6. The syenitic rocks are enriched in LILE and HFSE and exhibit normalized trace element patterns with negative Ba, Sr, and Ti due to fractionation of plagioclase and Ti-oxide minerals. On the other hand, rocks of the essexitic gabbros are more enriched in both LREE and HREE with a strong negative HF anomaly with low Yb and Lu, suggestion the presence of residual garnet in the mantle source.

Acknowledgement

We would like to thank Prof. Nikolai V. Vladykin, Head of the Laboratory of Geochemistry of Alkaline Rocks, Institute of Geochemistry, Russian Academy of Sciences, Irkutsk, Russia; for his help to do chemical analysis to complete this study.

References

[1] Bailey, D. K., Macdonald, R., 1970. Petrochemical variations among mildly peralkaline (comendite) obsidians from the oceans and continents. Contributions to Mineralogy and Petrology. 28, 340-351.

[2] Balashov, Y. A., Glaznev, V. N., 2006. Cycles of alkaline magmatism. Geochemistry International. 44, 274-285.

[3] Blatt, H., Tracy, R. J., 1995. Petrology: Igneous, Sedimentary, and Metamorphic. W. H. Freeman, New York.

[4] Bonin, B., 2007. A-type granites and related rocks: evolution of a concept, problems and prospects. Lithos. 97, 1-29.

[5] Cox, K. G., et al., 1979. The interpretation of igneous rocks. George Allen and Unwin London, Boston.

[6] de Gruyter, P., Vogel, T. A., 1981. A model for the origin of the alkaline complexes of Egypt. Nature. 291, 571-574.

[7] De Gruyter, P. C., (1983), The petrogenesis and tectonic setting of the Egyptian alkaline complexes. Michigan State University, 1983.

[8] Edgar, A. D., 1964. Phase-Equilibrium Relations in the System Nepheline-Albite-Water at 1,000Kg/Cm^2. The Journal of Geology. 72, 448-460.

[9] EL Ramly, M. F., et al., A petrological study on the central part of Gabal Abu Khruq Ring Complex, South Eastern Desert of Egypt. Vol. 51. Geol Survey Egypt, 1969.

[10] EL Ramly, M. F., et al., The alkaline rocks of South-Eastern Egypt. Egyptian Geol. Surv., Vol. 53, 1971.

[11] EL Ramly, M. F., Hussein, A. A., 1985. The Ring Complexes of the Eastern Desert of Egypt. J. Afr. Earth Sci. 3, 77-87.

[12] Foland, K. A., Henderson, C. M. B., 1976. Application of age and Sr isotope data to the petrogenesis of the Marangudzi ring complex, Rhodesia. Earth and Planetary Science Letters. 29, 291^301.

[13] Foland, K. A., et al., 1993. Formation of cogenetic quartz and nepheline syenites. Geochimica et Cosmochimica Acta. 57, 697-704.

[14] Fudali, R. F., 1963. Experimental studies bearing on the origin of pseudoleucite and associated problems of alkalic rock systems. Bull. geol. Soc. Am.. 74, 1101-1126.

[15] Garson, M. S., Krs, M., 1976. Geophysical and geological evidence of the relationship of Red Sea transverse tectonics to ancient feature. Geologic Soc. Am. Bull.. 87, 169-181.

[16] Giret, A., et al., 1980. Amphibole compositional trends in oversaturated alkaline plutonic ring-complexes. Canadian Mineralogist. 18, 481-495.

[17] Goldschmidt, V. M., 1954. Geochemistry. Clarendon Press, Oxford.

[18] Hamilton, D. L., MacKenzie, W. S., 1965. Phase-equilibrium studies in the system NaAlSiO4 (nepheline)^KAlSiO$_4$ (kalsilite)^ SiO$_2^H_2$O. Mineralogical Magazine. 34, 214-231.

[19] Harris, C., et al., 1999. Petrology of the alkaline core of the Messum Igneous Complex, Namibia: Evidence for the progressively decreasing effect of crustal contamination. Journal of Petrology 40, 1377-1397.

[20] Heier, K. S., 1964. Geochemistry of the nepheline syenite on Stjernoy, North Norway. Norsk Geol. Tidsskr. 44, 205-215.

[21] Kogarko, L. N., Petrogenesis. Role of volatiles. In: Sørensen, H., Eds.), The Alkaline Rocks. J. Wiley and Sons, London, 1974, pp. 474-487.

[22] Kyle, P. R., 1981. Mineralogy and Geochemistry of a Basanite to Phonolite Sequence at Hut Point Peninsula, Antarctica, based on Core from Dry Valley Drilling Project Drillholes 1, 2 and 3. Journal of Petrology. 22, 451-500.

[23] Landoll, J. D., et al., 1994. Nd isotopes demonstrate the role of contamination in the formation of coexisting quartz and nepheline syenites at the Abu Khruq Complex, Egypt. Contributions to Mineralogy and Petrology. 117, 305-329.

[24] Lutz, T. M., et al., 1988. The strontium and oxygen isotopic record of hydrothermal alteration of syenites from the Abu Khruq complex, Egypt. Contributions to Mineralogy and Petrology. 98, 212-223.

[25] Maniar, P. D., Piccoli, P. M., 1989. Tectonic discrimination of granitoids. Geological Society of America Bulletin. 101, 635-643.

[26] McKenzie, D., 1985). The extraction of magma from the crust and the mantle. Earth and Planetary Science Letters. 74, 81-91.

[27] Middlemost, E. A. K., 1975. The basalt clan. Earth Sci. Rev. 11, 337-364.

[28] Miyashiro, A., 1978. Nature of alkaline volcanic series. Contributions to Mineralogy and Petrology. 66, 91-104.

[29] Neary, C. R., et al., 1976. Granitic association of North Eastern Sudan. Geol. Soc. Am. Bull. 87, 1501-1512.

[30] Nickel, K. G., 1986. Phase equilibria in the system SiO_2–MgO–Al_2O_3–CaO–Cr_2O_3 (SMACCR) and their bearing on spinel/garnet lherzolite relationships. Neues Jahrbuch fur Mineralogic Abhandlungen 155, 259-287.

[31] Pearce, J. A., et al., 1984. Trace element discrimination diagrams for the tectonic interpretation of granitic rocks. J. Petrol.. 25, 956-983.

[32] Peters, T., et al., 1966. The melting of analcite solid solutions in the system $NaAlSiO_4$-$NaAlSi_3O$ $8H_2O$. American Mineralogist. 51, 736753.

[33] Serencsits, C. M., et al., 1981. Alkaline ring complexes in Egypt: Their ages and relationship in time. Journal of Geophysical Research: Solid Earth. 86, 3009-3013.

[34] Spera, F. J., 1981. Carbon Dioxide in Igneous Petrogenesis II: Fluid dynamics of mantle metasomatic processes. Contrib Mineral Petrol 77, 56-65.

[35] Sun, S. S., 1982. Chemical composition and origin of the Earth's primitive mantle. Geochim. Cosmochim. Acta. 46, 179-192.

[36] Sun, S. S., McDonough, W. F., Chemical and isotopic systematics of oceanic basalts: implications for mantle composition and processes. In: A. D. Saunders, M. Norry, Eds.), Magmatism in Ocean Basins. Geological Society of London Special Publication, London, 1989, pp. 313e345.

[37] Tuttle, O. F., Bowen, N. L., 1958. Origin of Granite in the Light of Experimental Studies in the System $NaAlSiO_4$^$KAlSiO_4$^SiO_2^H_2O. Geological Society of America, Memoirs. 74.

[38] Wilson, M., 1989. Igneous Petrogenesis. Unwin Hyman Ltd., London.

[39] Yoder, H. S. J., Tilley, C. E., 1962. Origin of basalt magmas. Journal of Petrology. 3, 342-532.